Nuclear Instruments and Methods in Physics Research A 332 (1993) 521–528
North-Holland

NUCLEAR INSTRUMENTS & METHODS IN PHYSICS RESEARCH
Section A

Neutron response of an ^{3}He proportional counter

E. Dietz, M. Matzke, W. Sosaat, G. Urbach and M. Weyrauch
Physikalisch-Technische Bundesanstalt, D-W-3300 Braunschweig, Germany

Received 17 February 1993

Response functions of cylindrical ^{3}He proportional counters are determined. The wall effect is calculated and the resolution function is obtained from measurements at neutron energies of 186 eV, 24 and 144 keV. The resolution function turns out to be a Gaussian slightly modified by an asymmetry correction. The response functions obtained agree well with measured responses. To show how they can be applied, a neutron spectrum measured at a filtered reactor beam is unfolded. This neutron spectrum is in agreement with transmission calculations for the neutron filters. Unfolding problems encountered are discussed in some detail.

1. Introduction

^{3}He proportional counters are widely used for detection and measurement of slow neutrons. Calculations of the response function of such counters were published already more than 20 years ago [1]. For fast neutrons, past work has concentrated on ^{3}He ionization chambers [2]. The ionization chamber has a significantly better resolution than a proportional counter. On the other hand, due to its construction the ^{3}He ionization chamber is more complex than a proportional counter, so a precise determination of its response function is not easy. The response functions published are not entirely satisfactory [2].

However, for medium energy neutrons ($E_n < 2$ MeV) the resolution of a proportional counter may suffice for practical measurements. The objective here is to study such a device in some detail and to determine its response functions. The proportional counters were mounted perpendicularly to collimated filtered neutron beams so that the ends of the counting wires were exposed neither to the beam nor to reaction products.

As a complete calculation of the response function of the detectors is not possible, only the wall effect is calculated on the basis of nuclear reaction data, range data for the reaction products and the geometry of the detectors. The result of this calculation is termed "ideal" response function in this paper. The "ideal" response function is then folded with an experimentally determined resolution function to account for statistical and other effects of the gas dynamics. This procedure allows response functions to be constructed which agree rather well with measured response functions at selected energies. The resolution function is then parametrized by a simple analytic ansatz and interpolated and extrapolated to energies at which experiments have not been made.

The validity of this procedure is then checked by unfolding measured spectra from filtered reactor beams. The unfolding poses numerous problems which will be investigated here. One of the most critical of these problems is the fact that the interpolated and extrapolated response functions are, of course, not entirely correct, but the unfolding codes available to us react very sensitively to even slightly incorrect input. Suggestions on how to handle this and related numerical problems are discussed in some detail.

It has been found that a ^{3}He proportional counter can be profitably used as a neutron spectrometer for neutron energies below 2 MeV with an energy resolution which is comparable to that of a recoil proton proportional counter. However, for an absolute determination of neutron fluences the ^{3}He proportional counter is unfortunately less precise than a recoil proton proportional counter, since the ^{3}He absorption cross section is less well known than the neutron–proton scattering cross section.

2. Calculation of the "ideal" response function

Two elementary nuclear processes contribute predominantly to the neutron response of a ^{3}He proportional counter: ^{3}He breakup into proton (p) and triton (T) with the differential cross section $d\sigma_{np}/d\Omega_p$ ($Q =$ 764 keV) and elastic neutron scattering (el) with the differential cross section $d\sigma_{el}/d\Omega_n$. Accordingly, the "ideal" response function $W(E, E_n)$ is a sum of two contributions, $W(E, E_n) = W_{np}(E, E_n) + W_{el}(E, E_n)$,

$$W_{np}(E, E_n) = \int d^3r\rho(\boldsymbol{r}) \int d\Omega_p \; \delta\big(E - E_{dep}(\boldsymbol{r}, \Omega_p, E_n)\big) \frac{d\sigma_{np}}{d\Omega_p}(E_n), \tag{1a}$$

$$W_{el}(E, E_n) = \int d^3r\rho(\boldsymbol{r}) \int d\Omega_n \; \delta\big(E - E_{dep}(\boldsymbol{r}, \Omega_n, E_n)\big) \frac{d\sigma_{el}}{d\Omega_n}(E_n). \tag{1b}$$

The quantity E represents the energy deposited in the counter. The reaction products may not be able to deposit their total energy in the counter before they are stopped by the counter wall. This wall effect is described in the function E_{dep}, which will be discussed in some detail below; it is dependent on the neutron energy E_n, the scattering geometry and the counter geometry. If the wall was absent, $W_{np}(E, E_n)$ would be proportional to a delta function at $E = E_n + Q$ and $W_{el}(E, E_n)$ would be proportional to $\theta(3E_n/4 - E)$ [$\theta(x) = 0$ for $x < 0$ and $\theta(x) = 1$ for $x \geq 0$].

The ^3He density $\rho(\boldsymbol{r})$ and the neutron energy are such that the mean free path of a neutron is much larger than the counter dimensions. The neutrons then interact homogeneously over the whole counter volume with the ^3He gas, and multiple scattering can be neglected. Reactions in the counter wall are not taken into account. The $\boldsymbol{r}$ integration extends over all possible interaction points. The five-dimensional integrals in eqs. (1a) and (1b) are determined numerically by a Monte Carlo integration.

The charged reaction products, i.e. recoiling ^3He nuclei in the case of elastic scattering or protons and tritons in the case of breakup, lose their energy in the filling gas in atomic processes and create electrons along their tracks. These electrons are collected and produce a signal proportional to the energy E_{dep} deposited in the filling gas. Gas amplification is assumed

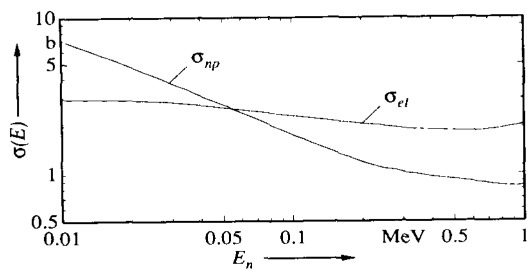

Fig. 1. ^3He(n, p) and elastic cross sections from the ENDF-B/VI nuclear data file [4].

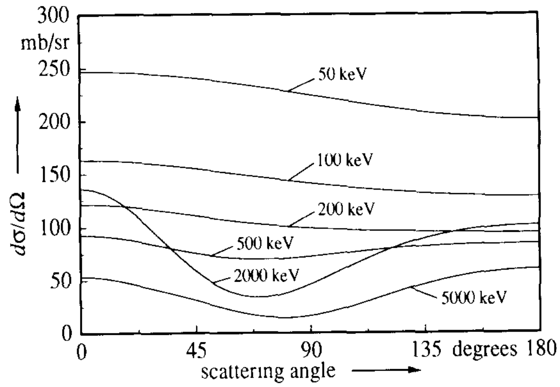

Fig. 2 Differential cross section versus scattering angle of the reaction ^3He(n, p)T in the laboratory frame. Each curve is labelled with the laboratory energy of the incoming neutron.

to be constant over the whole counter volume. The function E_{dep} can be calculated for a given geometry of the counter volume, if the range of the charged particle in the filling gas is known. Ranges are calculated from data collected by Ziegler [3].

The differential cross sections $d\sigma_{el}/d\Omega$ and $d\sigma_{np}/d\Omega$ are obtained from experimental data. Here it is assumed that the elastic cross section is isotropic in the center-of-mass (CM) frame $d\sigma_{el}/d\Omega_{CM} = \sigma_{el}/4\pi$. The total cross section σ_{el} is taken from the ENDF-B/VI data file [4]. Fig. 1 shows these data. The CM differential cross section for ^3He breakup into p and T is not isotropic even for neutron energies as low as 50 keV; it is calculated from data [5] of the inverse reaction T(p, n)^3He using the principle of detailed belance. Details of this calculation can be found in ref. [6]. In fig. 2 some typical cross sections are plotted.

3. Determination of the response function

The calculated function $W(E, E_n)$ is folded with the resolution function $P(E_c, E)$ of the detector to obtain

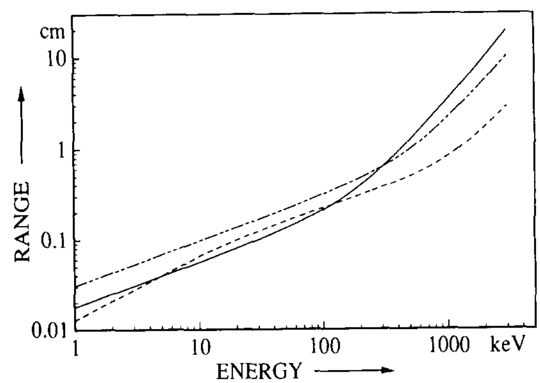

Fig. 3. Ranges in the mixture of 26.7 kPa of ^3He and 74.7 kPa Ar calculated from data by Ziegler [3]. Full line: proton ranges, short dashed: triton ranges, long dashed: ^3He ranges.

the response function $R(E_c, E_n)$ of the counter. The resolution function describes the probability density that an event releasing energy E in the counter will be registered at E_c,

$$R(E_c, E_n) = \int \mathrm{d}E\, P(E_c, E) W(E, E_n). \tag{2}$$

The resolution function cannot easily be calculated and must be determined experimentally. It is shown in the following that this resolution function can be parametrized by a Gaussian folded with an asymmetry correction.

For a parallel incident neutron beam with the spectral fluence $\Phi_E(E_n)$, the event density $Z(E_c)$ registered by the proportional counter is then given by

$$Z(E_c) = \int \mathrm{d}E_n R(E_c, E_n) \Phi_E(E_n). \tag{3}$$

For practical calculations this will be discretized on a suitable energy grid,

$$Z_k = \sum_l R_{kl} \Phi_l, \tag{4}$$

where Φ_l is the neutron fluence in the energy group between E_n^l and $E_n^l + \Delta E_n^l$. Analogously,

$$Z_k = \int_{\Delta E_c^k} \mathrm{d}E_c Z(E_c), \tag{5}$$

is the number of events in channel k between E_c^k and $E_c^k + \Delta E_c^k$, and

$$R_{kl} = \int_{\Delta E_n^l} \mathrm{d}E_n \int_{\Delta E_c^k} \mathrm{d}E_c R(E_c, E_n)/\Delta E_n^l, \tag{6}$$

is the response matrix. Comparing the response function $R(E_c, E_n)$ with experimental data allows the resolution function $P(E_c, E)$ in eq. (2) to be determined, if the shape of the incoming neutron spectrum $\Phi_E(E_n)$ (see eq. (3)) is known.

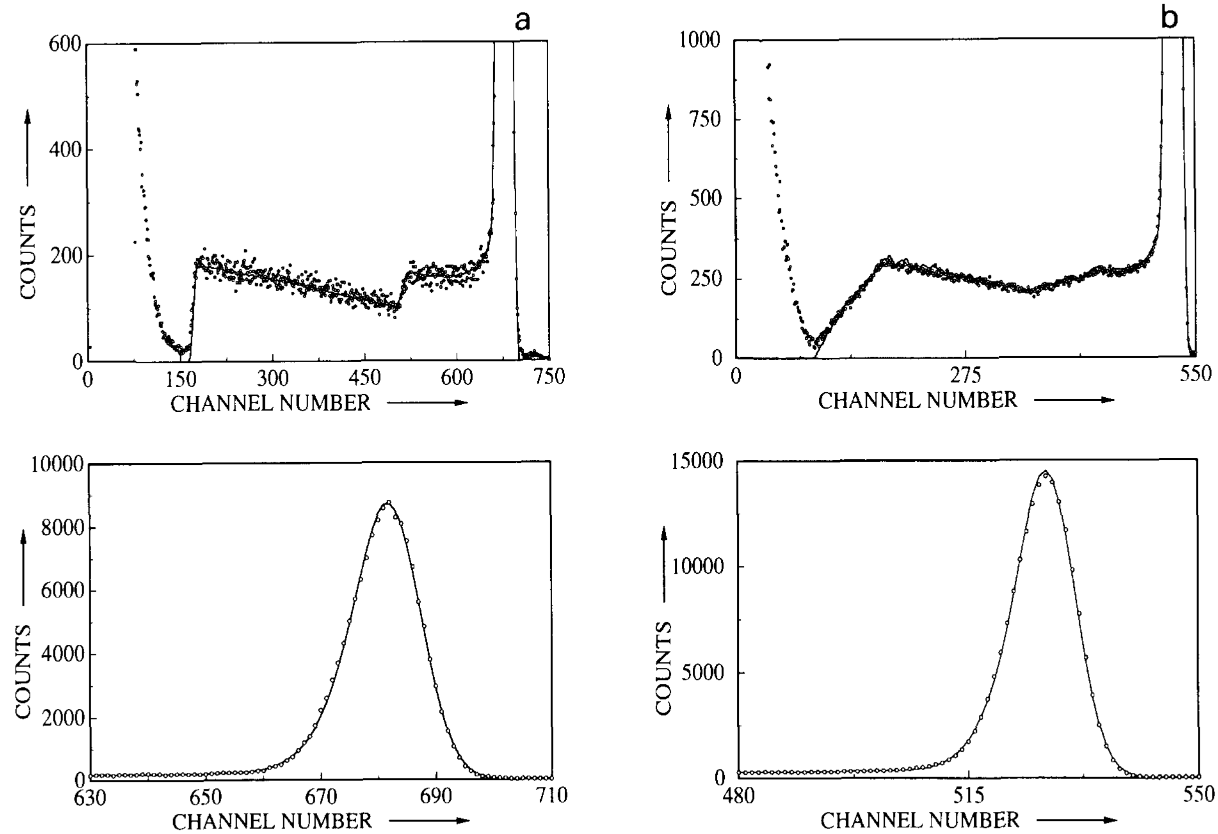

Fig. 4. (a) Response function (full line) compared with the measurement (circles) with the 2 in. ^{3}He counter for $E_n = 186$ eV. Top: wall effect region. Bottom: peak region. The channel width is 1.12 keV/channel. (b) The same as (a), but $E_n = 24$ keV and the channel width is 1.50 keV/channel. (c) Same as (a), but $E_n = 144$ keV and the channel width is 1.14 keV/channel.

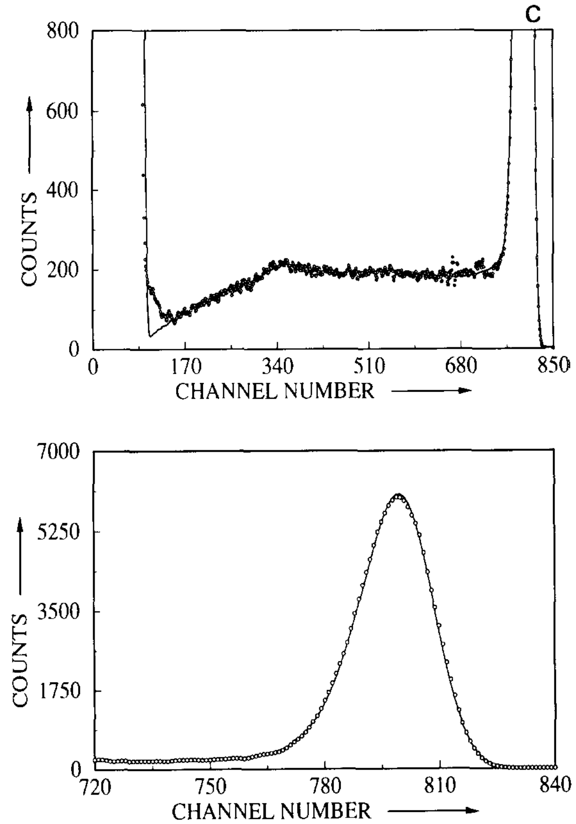

Fig. 4. (continued).

In practice three relatively narrow neutron lines with energies $E_n = 186$ eV, $E_n = 24$ keV and $E_n = 144$ keV are employed for this purpose. They are produced at the reactor of the Physikalisch-Technische Bundesanstalt (PTB) with suitable filters, and the Φ_i are assumed to be known from transmission calculations for these filters [9]. This assumption is valid for narrow single peaks if the reactor spectrum entering the filter is flat enough in the energy range of the peak. This should hold true for the narrow peaks at 186 eV and 24 keV; for the 144 keV line the peak width is rather large and variations of the reactor spectrum within the peak energy range cannot be excluded. The neutron peaks are slightly asymmetric towards lower energies with a full width at half maximum (FWHM) of about 1.7 keV (24 keV line) and about 8 keV (144 keV line). Experimental details are discussed in the following section.

The resolution function is assumed to be a Gaussian $G(E_c, E)$ with an asymmetry correction ($G(E_c, E) = e^{-(E_c-E)^2/(2s^2)}/\sqrt{2\pi}s$). The width of the Gaussian is parametrized by

$$s^2(E) = a + bE + cE^2. \tag{7}$$

A triangular form was assumed for the asymmetry, i.e. a fraction p of all events falling into an energy interval ΔE at energy E is distributed triangularly into the energy interval (E_0, E) with $E_0 = E(1-\alpha)$. The resolution function $P(E_c, E)$ is then given by

$$P(E_c, E) = \int_{E_0}^{E} \mathrm{d}E' G(E_c, E') \left[(1-p)\delta(E-E') + p \frac{2}{(E-E_0)^2}(E'-E_0) \right], \tag{8}$$

and is therefore characterized by five parameters a, b, c, p and α, which should be energy independent.

Two cylindrical ^{3}He counters are used for the measurements: a 2 in. counter (diameter 5.08 cm) filled with 26.7 kPa of ^{3}He and 74.7 kPa of argon and CO_2, and a 1 in. counter (diameter 2.54 cm) with 400 kPa of ^{3}He and 350 kPa of krypton. Both have walls of stainless steel and an active length of about 30 cm. An additional cadmium shielding 1 mm thick is used. The pressure of the krypton admixture in the 1 in. counter is not precisely known, so it is estimated by comparing calculated response functions with various pressures and the measurement of the 144 keV line. Fig. 3 shows ranges of protons and tritons calculated from data by Ziegler [3] for the gas mixture of the 2 in. counter.

In figs. 4 and 5, measured and constructed response functions are compared for the 2 in. counter and the 1 in. counter, respectively. The parameters for the 2 in. counter are $a = 1.8$ keV^2, $b = 3.25 \times 10^{-2}$ keV, $c = 1.35 \times 10^{-5}$, $p = 0.3$ and $\alpha = 0.028$, and for the 1 in. counter $a = 6.5$ keV^2, $b = 5.4 \times 10^2$ keV, $c = 2.7 \times 10^{-5}$, $p = 0.37$ and $\alpha = 0.035$. Estimated relative standard deviations are about 10% for each parameter. The agreement between measured and constructed response is quite good, wall effect and peak-to-total ratio being exactly reproduced. The χ^2 values per degree of freedom in the peak region are about 3.

Frankly, the results presented in figs. 4 and 5 might even be too good and somewhat misleading, since they wrongly suggest that the response function can be determined precisely. This is certainly not true considering the approximations and the *fitting* procedure involved. In principle, it would be necessary to associate an uncertainty band with the response functions. But even if uncertainties were assigned to the response functions the validity of the parameters a, b, c, p and α at energies above 144 keV could only be determined if a precisely known neutron spectrum were available.

4. Experimental setup and investigation of the asymmetry

In this section the resolution function and its experimental determination will be studied in more detail.

As already mentioned filtered neutron beams were used for the measurements of the response functions [7]. The beams are well collimated; the FWHM perpendicular to the beam is about 8.5 cm at the point of measurement. The diameter at the base of the beam profile is about 15 cm. The cylindrical counters were adjusted perpendicularly to the beam and centered so that the ends of the counting wires were not exposed to the beam or the charged reaction products. Neutrons with energies of at least a few hundred eV for measuring the response function have the advantage that the distribution of reactions in the counting volume is homogeneous.

The 186 eV line from a uranium-filtered beam is contaminated by about 20% of a 100 eV line and a very small higher energy contribution. The 24 keV beam was realised with the combination of an iron, aluminum and sulphur filter using a titanium disk as a difference filter to suppress the higher energy contamination. The spectrum at 24 keV is a difference spectrum of measurements with and without the titanium disk. This difference spectrum contains only 1.5% of higher energy neutrons. An unresolved part of an epithermal contribution of about 3% is removed by subtracting an epithermal spectrum. This spectrum is measured with the counter positioned 20 cm away from the beam axis. It is assumed that the epithermal intensity is nearly the same in this position as in the center position. The 144 keV beam is obtained from a silicon filter combined with 60 mm of titanium which suppresses the 54 keV contamination to 0.2% of the 144 keV intensity. As the peak of the epithermal response is well separated from the 144 keV, this fraction is easily subtracted.

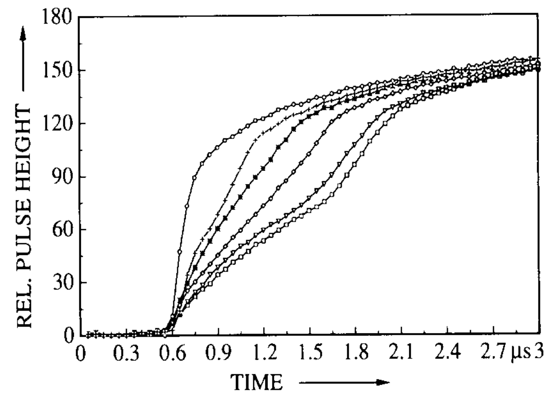

Fig. 6. Typical pulse shapes of the preamplifier pulses of the 2 in. ^3He counter irradiated with 144 keV neutrons. The pulses are measured with a digital storage oscilloscope and selected for the same pulse height.

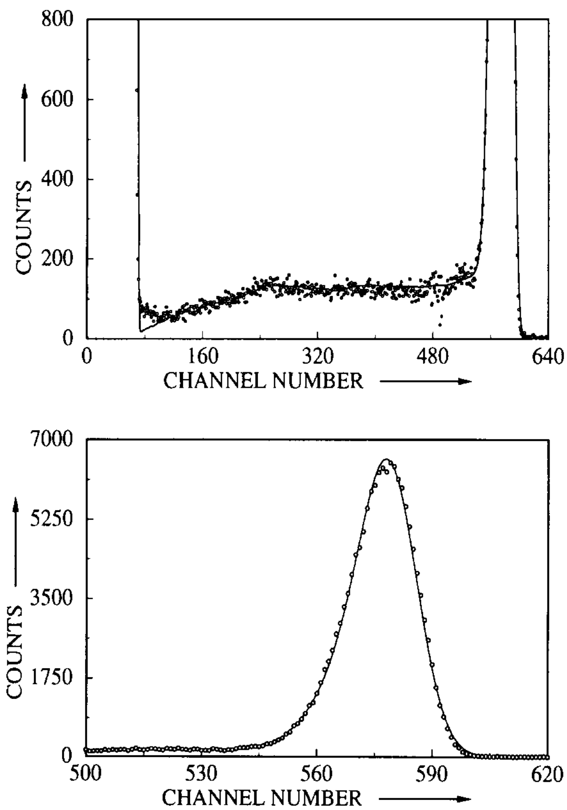

Fig. 5. Response function (full line) compared with the measurement with the 1 in. ^3He counter for a neutron energy of 144 keV. Top: wall effect region. Bottom: peak region. The channel width is 1.57 keV/channel.

Commercially available electronics was used for the measurements. A charge-sensitive preamplifier coupled with a short cable to the proportional counter and a main amplifier with the time constant set to 8 μs (peaking time = 16 μs) and unipolar output. The relatively high time constant is necessary to compensate for the varying rise times of the pulses (see fig. 6). The high voltage was adjusted to minimize the asymmetry of the peak together with the value of the FWHM. Count rates were between 10/s and 150/s. The measured spectra must be corrected for zero level of the analog-to-digital converter and the amplifiers. This was done using a precision pulser to find the position of the zero channel. The energy scale of measurement is assumed to be linear.

Increasing the voltage of the proportional counter results in increased asymmetry whereas decreasing it leads to higher values of the FHWM. The peak broadening is mainly due to statistical fluctuations in the gas amplification, recombination and electronic noise. These effects should lead to a Gaussian broadening only. The physical reason for the asymmetry is not understood in detail. A possible reason may be that tracks of the reaction products with a direction almost perpendicular to the wire suffer an increased effect of space charge shielding. This results in a decreased gas amplification near the wire and a reduction of the amplitude of the pulses. Fig. 7 shows the increasing asymmetry with increasing voltage for the 2 in. counter.

In an attempt to clarify the nature of this asymmetry, the rise time and the shape of the pulses at the output of the preamplifier were analysed. Tracks which are formed almost perpendicularly to the wire should have longer rise times than those parallel to it. Single preamplifier pulses of the 2 in. counter were therefore stored in a digital storage oscilloscope. The time scale of the oscilloscope was set to 50 ns sampling time, and the amplitude was sorted into an 8 bit scale. A high voltage of 1050 V was applied. A measurement was made with 144 keV neutrons and about 25000 pulses from the peak region were stored and analysed for pulse shape and amplitude.

Some examples of pulse shapes are shown in fig. 6, demonstrating the different rise times and the varying shapes in the initial part of the pulses. The two steps showing up in the pulses with longer rise times are due to protons and tritons whose ionization charges (with maximum ionization density at the end of each track) reach the counting wire at different times. All pulses in this figure are selected so as to have the same amplitude, which was taken as the mean value between 5 and 15 μs after the initial rise of each pulse. This rather long interval had to be chosen due to the restriction of the large amplitude steps of the storage oscilloscope (8-bit). With this averaging procedure it was possible to enhance the resolution of the pulse height sorting to about 12 bit.

To look for possible correlations between the pulse shape and pulse height of the pulses $g(t)$ from the preamplifier, the first moment M_1 of the derivative

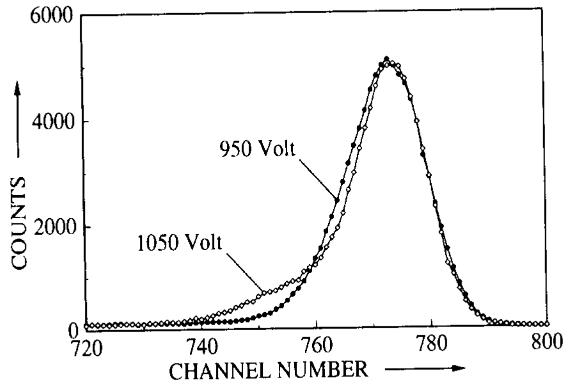

Fig. 7. Pulse height spectra of the 2 in. ^{3}He counter with high voltages of 950 and 1050 V demonstrating the increasing asymmetry of the peaks. The spectra are taken by irradiating the counter with 186 eV neutrons from the uranium-filtered beam. The amplification was adjusted for the same position at the right-hand side of the peaks.

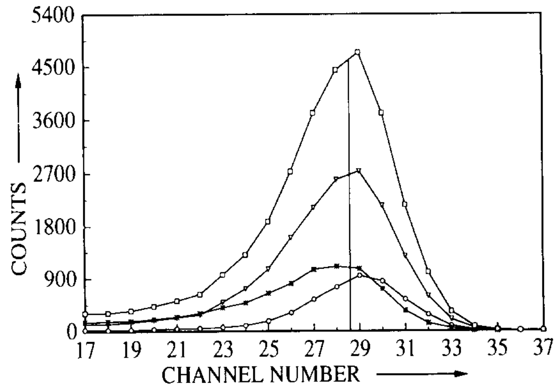

Fig. 8. Pulse height spectra at $E_n = 144$ keV in the peak region. Pulses from the digital storage oscilloscope are sorted into different M_1 intervals (see eq. (9)). circles: $M_1 = 460$ to 660 ns, triangles: $M_1 = 660$ to 860 ns, stars: $M_1 = 860$ to 1290 ns, squares: $M_1 = 460$ to 1290 ns.

$g'(t)$ was calculated in the time interval from $t_0 = 0$ μs to $t_1 = 3$ μs,

$$M_1 = \int_{t_0}^{t_1} g'(t)t \, dt \Big/ \int_{t_0}^{t_1} g'(t) \, dt; \tag{9}$$

M_1 corresponds to the "time centre" of the collected charge. For selected M_1 intervals the corresponding amplitude spectra of the peak region are shown in fig. 8. It demonstrates that long rise times, i.e. large values of M_1, are weakly correlated to an enhanced asymmetry of the peak. This supports the idea that the asymmetry in the pulse height spectra of a ^{3}He proportional counter is a space charge effect. This effect could possibly be seen more clearly with strictly monoenergetic neutron lines.

5. Application: neutron fluence determination by unfolding

It can be summarized from the results in section 2 that the response matrix R_{kl} (eq. (4)) determined by folding the function $W(E, E_n)$ with $P(E_c, E)$ agrees well with experimental results at the quasi-monoenergetic lines investigated, if the parameters of $P(E_c, E)$ are properly chosen.

To unfold neutron spectra in the energy range up to $E_n = 1.4$ MeV, R_{kl} must be known for $E_n < 1.4$ MeV and $E_c < (1.4 + 0.764)$ MeV on a suitable energy grid. $P(E_c, E)$ must be extrapolated using the parameters determined at low energies. In view of the fact that there is a rather large uncertainty connected with shape of the asymmetry correction, and to reduce the numerical effort, the asymmetry correction was neglected for the unfolding. Since the asymmetry correction contributes significantly only in a small energy interval around the nominal energy E, it is expected that only the fine structure of the neutron spectra will not be correctly reproduced in an unfolding without asymmetry. The parameters a, b, c of the resolution function, however, are slightly different from the values obtained with asymmetry correction.

The least-squares adjustment to determine the parameters of the width function $s(E)$ was therefore performed again for the 2 in. counter using lines produced with a natural iron filter. Again, it was assumed that the shape of Φ_t in each energy interval was equal to that of the calculated transmission function [9]. The second-order polynomial approximation for $s^2(E)$ in eq. (7) fitted well in the entire energy range below 1864 keV. For the FWHM at energies of 764, 908 and 1864 keV, values of 16.8, 18.6 and 31.6 keV were found, respectively. The corresponding parameters $a = 14.5$ keV^2, $b = 0.0191$ keV, $c = 3.74 \times 10^{-5}$ determine $s(E)$ in the entire energy range. With these parameters of the width function the overall response function R_{kt} was calculated using the energy calibration obtained for the 24 keV peak of the measured spectrum. The energy grid was chosen in 1 keV steps for E and E_n.

Uncertainties of R_{kt} were not taken into account for the unfolding, i.e. R_{kt} was assumed to be precisely known, and the Φ_t were assumed to be entirely unknown, i.e. no a priori information about the neutron spectra was assumed. The determination of Φ_t by unfolding of eq. (4) was performed by minimizing the χ^2 expression

$$\chi^2(\Phi_1, \ldots, \Phi_M) = \sum_k \left(Z_k - \sum_t^M R_{kt}\Phi_t \right)^2 / \sigma_k^2, \tag{10}$$

with respect to Φ_t. σ_k^2 is the variance of Z_k estimated as $\sigma_k^2 = Z_k$ assuming Poisson statistics. The SAND-II algorithm [8] was used for the minimization.

The unfolding of the neutron fluence of the PTB's natural iron filter was performed in three adjacent neutron energy intervals, beginning at high energies (700 keV $< E_n <$ 1400 keV), folding the resulting Φ_t with R_{kt}, and subtracting these results from Z_k to obtain the "measured" spectrum without high energy contributions for neutron energies below 700 keV. For the second interval (50 keV $< E_n <$ 700 keV) and the third interval ($E_n <$ 50 keV) the same procedure was followed. The measured spectrum for $E_k >$ 764 keV was used as input spectrum for the SAND-II calculations.

The result for Φ_t in the entire energy range considered is shown in fig. 9. The lower curve with an inverted ordinate is the calculated transmission function of 672 mm natural iron [9], the upper curve shows the unfolded neutron spectrum. This result was obtained after several thousand iteration steps of the SAND-II algorithm in each neutron energy interval.

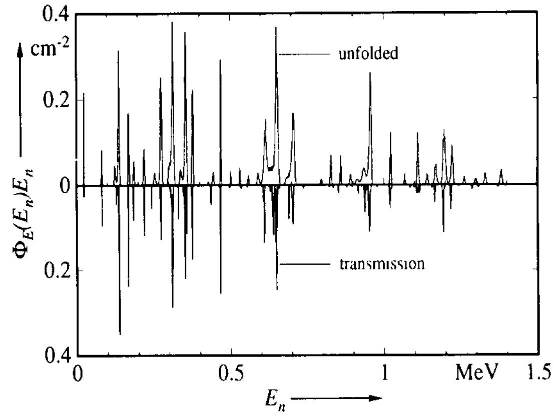

Fig. 9. Spectral fluence times neutron energy E_n for the natural iron filter of the PTB. Upper curve: SAND-II unfolding results using R_{kt} matrices and the measured spectrum Z_k for $E_k >$ 764 keV as SAND-II input. Lower curve: Calculated transmission spectrum for the filter not taking into account the incoming reactor spectrum. Both spectra are properly scaled.

Both spectra are properly scaled. Absolute fluence determination, however, would be possible if the real number of ^{3}He particles in the counter were taken into account. A comparison of the two spectra shows that the energy calibration performed by means of the 24 keV peak of the measured spectrum is obviously correct, which means that a linear transformation between channel number and energy E_k is valid within the uncertainties. From the width of the unfolded peaks above 0.5 MeV it may be concluded that the FWHM values used to evaluate R_{kt} are possibly too small. The amplitudes of Φ_t are not expected to agree with those of the transmission function due to the unknown reactor neutron spectrum entering the filter.

In fig. 10 the measured spectrum is compared with the refolded result obtained by means of eq. (4). The energy scale is in neutron energies ($E_n = E_c - E_0$ with $E_0 = 764$ keV). The χ^2-value per degree of freedom ν for the refolded curve is below 1.0 for energies greater than 50 keV. For the 24 keV peak, however, a χ^2/ν value of 4.0 was obtained. This discrepancy is probably related to the neglecting of the asymmetry correction mentioned above. The good agreement between the two curves for energies $E_c - E_0 < 0$ again shows the consistency between calculated response functions and measured values.

From the unfolding work performed to determine neutron spectra at the PTB reactor filters it is concluded that

– the channel–energy relation for the ^{3}He proportional counter used can be considered as linear within an uncertainty of 0.3% for the energy value E_c. The

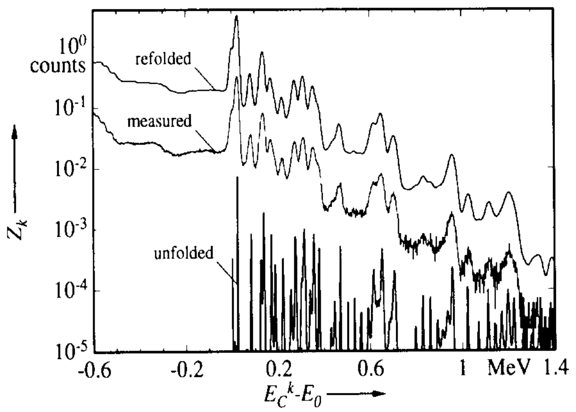

Fig. 10. Comparison of measured and refolded spectra according to eq. (4). To simplify the comparison the refolded spectrum is multiplied by a factor of 10. The unfolded fluence for the iron filter is also shown.

energy calibration may be performed by using the 24 keV peak;

– the energy dependent width $s(E)$ of the Gaussian resolution function can be approximated by the square root of a second-order polynomial in energy. The parameters of this polynomial must be determined by using a known neutron spectrum. The uncertainties of the $s(E)$ obtained at a given energy E are estimated to be about 10%.

The unfolding code reacts very sensitively to inconsistent input. Wrong response functions R_{kl} with wrong resolution functions may result in "unphysical" oscillations of the unfolded neutron spectrum. The error of the response function R_{kl} in a channel k should be smaller than the standard deviation of Z_k.

For some of the peaks investigated (e.g. the epithermal peak and the peak at 24 keV of the Fe filter) the χ^2/ν values obtained after refolding were too large. For these cases it was attempted to include the asymmetry correction mentioned above in the response function R_{kl}. These attempts, however, did not produce satisfactory results, although there was a slight reduction of χ^2. This may be explained by the fact that the uncertainties in the measured spectrum are small compared to possible uncertainties in the response functions. Unfortunately, it is likely that the response functions will never be determined precisely enough to match the precision of a measured spectrum Z_k.

In the future work it is necessary to quantitatively include the uncertainty of the R_{kl} matrices in the unfolding procedure in order to perform a complete uncertainty propagation. Unfolding attempts with the Monte Carlo code MIEKE [10] with increased uncertainties at those energies E_c where the measured and refolded spectrum strongly disagree, are in progress.

Acknowledgement

This work was supported in part by the Commission of the European Community (CEC) under contract BI7-0031-C.

References

[1] S. Shalev, Z. Fishelson and J.M. Cuttler, Nucl. Instr. and Meth. 71 (1969) 292.

[2] W.C. Sailor, S.G. Prussin and M.S. Derzon, Nucl. Instr. and Meth. A270 (1988) 527.

[3] J.F. Ziegler, The Stopping and Ranges of Ions in Matter (4 volumes) (Pergamon, 1977).

[4] ENDF-102, Data formats and procedures for the evaluated nuclear data file ENDF, P.F. Rose and C.L. Dunford (eds.), Brookhaven National Laboratory Upton, New York (1990).

[5] M. Drosg and O. Schwerer, Technical Report No. 273, IAEA, Vienna (1987).

[6] M. Weyrauch, report PTB-7.51-91-1, Physikalisch-Technische Bundesanstalt, Braunschweig (1991).

[7] W.G. Alberts and E. Dietz, PTB report FMRB-112, Braunschweig (1987).

[8] W.N. McElroy, S. Berg, T. Crockett and R.G. Hawkins, SAND-II, a Computer-Automated Iterative Method for Neutron Flux Spectra Determination by Foil Activation, Report AFWL-TR-67-41, US Air Force Weapons Laboratory (1967).

[9] M. Matzke, K. Knauf, E. Dietz, A. Plewnia and W.G. Alberts, Proc. 7th ASTM-EURATOM Symp. on Reactor Dosimetry, Strasbourgh (Kluwer Academic Publishers, Dordrecht, Boston, London, 1992) p. 377.

[10] K. Weise and M. Matzke, Nucl. Instr. and Meth. A280 (1989) 103.